

25 μL of the hybridoma supernatant into rows A1-A12, and is serially diluted 2-fold down the plate. The plate was allowed to incubate for 2 h at 37 $^{\circ}\text{C}$, which was then followed by a deionized water wash/shaking (10 times). All wells were next treated with 25 μL of a goat anti-mouse glucose oxidase (Cappel) solution, which was diluted previously 1:500 in Blotto. The plate was allowed to incubate for 1 h at 37 $^{\circ}\text{C}$. This was followed by (10 \times) deionized water wash/shaking. The plate is finally developed with 50 μL /well of a developing solution (25 mL, 0.2 M sodium phosphate, pH 6.0, 3 mL, 20% glucose/deionized water, 200 μL , 0.1% horseradish peroxidase/0.1 M phosphate buffer, pH 6.0, 200 μL , ABTS (BMB)) (45 mg/mL of deionized water). After 30 min the plate (each well) absorbance was determined at 405 nm on a Molecular Devices (V_{max}) kinetic plate reader.

A typical competition ELISA was performed in the following manner. A "limiting" antibody and antigen concentration as determined above is used in the following manner. The BSA-hapten conjugate (concentration determined above) in PBS is added at 25 μL /well to an ELISA plate. Methanol fix was added at 50 μL /well for 5 min. The methanol is removed, and the plate is air-dried for 10 min. The plate is blocked as described above with Blotto (50 μL /well) at 37 $^{\circ}\text{C}$ for 30 min, and the excess Blotto is removed. Next, the antigen (hapten) or substrate (diluted 1:20 in PBS-5% DMF) is serially diluted 2-fold (12 times). These solutions (12.5 μL) (each dilution) are added to the ELISA plate in the appropriate well, A1-A12, followed by the antibody (concentration determined above) (12.5 μL). This is allowed to incubate for 2 h at 37 $^{\circ}\text{C}$. The plates are washed with deionized water (10 \times), and goat anti-mouse glucose oxidase is added (described above) followed by incubation for 1 h at 37 $^{\circ}\text{C}$. The plate is again washed with deionized water (10 \times) followed by the addition of developing solution (described above). Absorbances are read at 405 nm.

The data (absorbances) obtained were fitted to eq 2 where CP is the absorbance determined and t is the antigen or substrate concentration. $P(1)$, $P(2)$, $P(3)$, and c are adjustable parameters in the four-parameter logistic fit.²⁵

$$\text{CP} = \frac{P(1)}{1 + P(2)t^c} + P(3) \quad (2)$$

Chemical Modification of Antibodies. (a) **Phenylglyoxal.** A 50- μL aliquot of a phenylglyoxal solution (6 mM, 125 mM NaHCO_3 , pH 7.5) was added to buffer (195 μL ; 125 mM, pH 7.5, NaHCO_3) containing antibody (20 μM). The mixture was vortexed and left to stand for 1 h at room temperature. This was then transferred to a microdializer (Pierce) and dialyzed with 125 mM pH 7.5 NaHCO_3 with a flow-through of approximately 150 mL/h for 2 h. This was then flushed with 4 \times 60 mL portions of pH 8.4 50 mM CHES-100 mM NaCl and left to stand in this buffer overnight. This was again flushed 3 \times 50 mL portions of pH 8.4 50 mM CHES-100 mM NaCl the next morning. Samples were removed, protein concentrations recalculated (BCA), and assays run for catalytic activity (HPLC) or binding (ELISA). A similar procedure was used with hapten present (200 μM).

(b) **Maleic Anhydride.** A 5- μL aliquot of a maleic anhydride solution (0.06 M, dioxane) was added to 229 μL of 20 mM pH 8.0 borate-100 mM NaCl containing 20 μM of antibody. The solution was vortexed and left to stand at room temperature for 1 h. This was then transferred to a microdializer and dialyzed as described above with 50 mM phosphate, pH 7-100 mM NaCl overnight, followed by 50 mM CHES, pH 8.4-100 mM NaCl for 2 h. Samples were removed, protein concentrations calculated (BCA), and assays run for catalytic activity or binding.

(c) **Diethyl Pyrocarbonate.** A 10- μL aliquot of a 0.6 M diethyl pyrocarbonate solution in ethanol is diluted in 1 mL of NaOAc (150 mM, pH 6-100 mM NaCl). Of this 5 μL is added to 229 μL of NaOAc (150 mM, pH 6.0-100 mM NaCl) containing 20 μM of antibody. The mixture is vortexed and left to stand at 4 $^{\circ}\text{C}$ overnight. This was then transferred to a microdializer and dialyzed as described above with CHES (50 mM CHES, pH 8.4-100 mM NaCl). Samples were removed, protein concentrations determined (BCA), and assays performed for catalytic activity and binding.

Acknowledgment. This work was supported in part by NIH Grant GM4385801. We thank Jo Ann Meyer for preparation of the manuscript.

(25) Ukraincik, K.; Pikkosh, W. *Methods Enzymol.* 1981, 74, 497.

Coupled Kinetic Analysis of Cleavage of DNA by Esperamicin and Calicheamicin

Hiroko Kishikawa, Ying-Ping Jiang, Jerry Goodisman, and James C. Dabrowiak*

Contribution from the Department of Chemistry, Center for Science and Technology, R 1-014, Syracuse University, Syracuse, New York 13244-4100. Received November 9, 1990

Abstract: A coupled kinetic analysis of esperamicin, calicheamicin, and DNase I cleavage of covalently closed circular PM2 DNA has been carried out. Analysis of the optical density data derived from agarose gel electrophoresis experiments shows that esperamicin A₁, like the hydrolytic enzyme DNase I, produces mainly single-strand breaks in DNA. These agents cause covalently closed circular form I DNA to be initially converted to nicked circular form II DNA. However, the ratio of the rate constant for this process (k_1') to that associated with conversion of form II to linear form III DNA (k_2') is not consistent with completely random nicking, and some double-strand cleavage may occur. The values of k_1'/k_2' found for DNase I and esperamicin A₁ were 5.4 and 3.9, respectively. The behavior of these agents sharply contrasts with that of esperamicin C and calicheamicin, for which double-strand cleavage of DNA is deduced from the analysis. Although the rate constant for introducing the first break in DNA for calicheamicin is lower than the corresponding rate constant for esperamicin C, the second break (in the opposing strand) is fast for calicheamicin, making it the better double-strand cleaving agent. These drugs are unique among antitumor agents in that a single activation event on the warhead portion produces a double-strand break in DNA without the need to posttreat the DNA with other agents in order to induce a cleavage. The cleavage kinetics are discussed in terms of the structural differences in these unusual anticancer drugs.

The newly discovered anticancer drugs esperamicin^{1,2} and calicheamicin^{3,4} (Figure 1) exhibit high potency against murine tumor lines. These compounds possess sugar groups appended to an unusual 1,5-diyne-3-ene core structure referred to as the "warhead". In the presence of reducing agents and DNA the

warhead undergoes a rearrangement to create a phenylene di-radical that causes strand breaks by attacking the sugar groups

(1) Golik, J.; Clardy, J.; Dubay, G.; Groenewold, G.; Kawaguchi, H.; Konishi, M.; Krishnan, B.; Ohkuma, H.; Saitoh, K.-I.; Doyle, T. W. *J. Am. Chem. Soc.* 1987, 109, 3461-3462. Golik, J.; Dubay, G.; Groenewold, G.; Kawaguchi, H.; Konishi, M.; Krishnan, B.; Ohkuma, H.; Saitoh, K.-I.; Doyle, T. W. *Ibid.* 1987, 109, 3461-3462.

* To whom correspondence should be addressed.

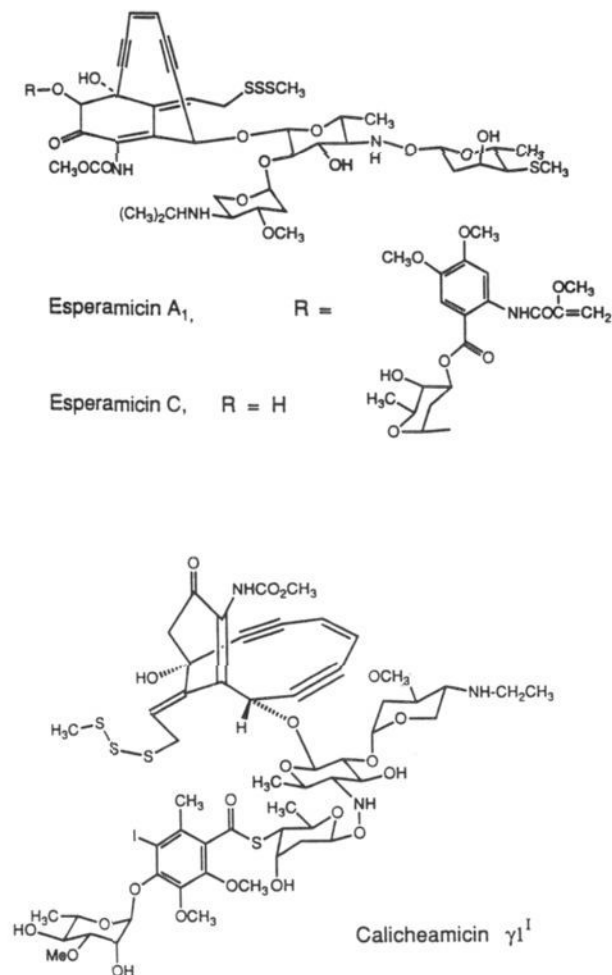


Figure 1. Structures of esperamicins A₁ and C and calicheamicin γ_1^1 .

of DNA. An interesting feature of esperamicin and calicheamicin as well as the chromophore of neocarzinostatin⁵ is that a single activation event produces 2 equiv of a species capable of reacting with sites on DNA, i.e., the phenylene diradical. This raises the possibility that a single drug molecule, after activation, can react with opposing strands to produce a double-strand break in DNA. Since this type of lesion is more difficult to repair than a single-strand peak, it is possible that a high frequency of double-strand breaks in DNA may be part of the basis for the extreme cytotoxicity of this unusual class of antitumor agent.

The evidence that esperamicin and calicheamicin cleave DNA via a double-strand process is primarily based on the drug-induced cleavage pattern on opposite DNA strands^{2,4} and in the case of calicheamicin on labeling experiments showing that both radicals of the phenylene diradical abstract hydrogen atoms from DNA.⁶ In the absence of additional information such as the absolute rate processes for cleavage on both strands, it is not clear whether a single activated "warhead" produces lesions on opposing strands, i.e., a double-strand peak, or whether the second peak is caused by a second drug binding to the nicked site and subsequently

(2) Long, B. H.; Golik, J.; Forenza, S.; Ward, B.; Rehffuss, R.; Dabrowiak, J. C.; Catino, J. J.; Musial, S. T.; Brookshire, K. W.; Doyle, T. W. *Proc. Natl. Acad. Sci. U.S.A.* **1989**, *86*, 2-6.

(3) Lee, M. D.; Dunne, T. S.; Siegel, M. M.; Chang, C. C.; Morton, G. O.; Borders, D. B. *J. Am. Chem. Soc.* **1987**, *109*, 3464-3466. Lee, M. D.; Dunne, T. S.; Chang, C. C.; Ellestad, G. A.; Siegel, M. M.; Morton, G. O.; McGahren, W. J.; Borders, D. B. *Ibid.* **1987**, *109*, 3466-3468.

(4) Zein, N.; Sinha, A. M.; McGahren, W. J.; Ellestad, G. A. *Science* **1988**, *240*, 1198-1201. Zein, N.; Poncin, M.; Nilakantan, R.; Ellestad, G. A. *Ibid.* **1989**, *244*, 697-699.

(5) Goldberg, I. H. *Free Radical Biol. Med.* **1987**, *3*, 41.

(6) Zein, N.; McGahren, W. J.; Morton, G. O.; Ashcroft, J.; Ellestad, G. A. *J. Am. Chem. Soc.* **1989**, *111*, 6888-6890.

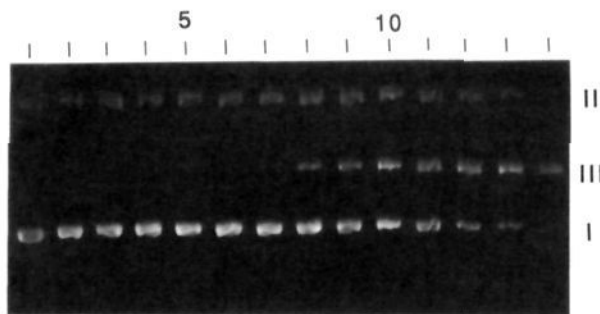


Figure 2. Photograph of agarose gel showing esperamicin C cleavage of PM2 DNA. The drug concentration in the various lanes, in order of increasing drug concentration (left to right), can be found in the Experimental Section. Lane 1 is zero drug concentration. The various forms of PM2 DNA, covalently closed circular (I), nicked circular (II), and linear (III), are shown on the right of the figure.

causing a break in the opposite strand. In the case of neocarzinostatin, a "double-strand" break is the result of a break in the sugar-phosphate backbone on one strand and the creation of an apurinic/apyrimidic site two nucleotides away from the initial break on the opposing DNA strand.⁷ Treatment of the modified DNA with endonuclease IV or putrescine, agents that attack apurinic/apyrimidic sites, is necessary in order to cause the second break in DNA.

In this paper we examine the ability of esperamicins A₁ and C and calicheamicin γ_1^1 to cleave closed circular PM2 DNA. The cleavage data are quantitatively analyzed with use of coupled kinetic models representing single- and double-strand cleavage processes. For comparative purposes, we also analyze cleavage of PM2 DNA by the hydrolytic enzyme DNase I under conditions previously reported to yield single-strand breaks in DNA.⁸

PM2 DNA, a covalently closed circular DNA molecule that is 9300 nucleotides long, is a convenient substrate for studying the cleavage action of DNA-nicking drugs. An agent capable of binding to DNA and yielding 1 equiv of a DNA-damaging group from a single activation event would cause an initial break in the PM2 genome, leading to the loss of supercoiling and the formation of nicked circular form II DNA. Subsequent binding and activation events would cause additional nicking of form II DNA. If two breaks on opposing DNA strands were relatively close to one another, the DNA segment between the breaks would "melt", causing form II to be converted to the linear form, form III DNA. Although DNA melting depends strongly on sequence as well as other factors,⁹ breaks on opposing strands up to 6-10 base pairs apart would likely cause linearization of the DNA molecule under the conditions used in this study.

Experimental Section

The esperamicins (esp) were obtained from J. Golik of Bristol-Myers Squibb Co., Wallingford, CT, while the sample of calicheamicin γ_1^1 was obtained from G. Ellestad of Lederle Laboratories. Stock drug concentrations ($\sim 3 \times 10^{-4}$ M) were made by dissolving weighed amounts of the drugs, 1-3 mg, in ethanol. Dilutions necessary for the strand scission work were done by adding a portion of the ethanol stock to a larger volume of the aqueous buffer used in the study. The maximum concentration of ethanol introduced by this procedure in any of the cleavage experiments was <1%. All DNA concentrations are stated in base pairs.

Cleavage of PM2 DNA. The cleavage of PM2 DNA by esperamicin and calicheamicin was carried out in a total volume of 13 μ L at 37 $^{\circ}$ C for 10 min in the buffer 6.2 mM Tris-HCl/0.6 mM EDTA, pH 7.5. To 2 μ L of the solution containing DNA was added 8 μ L of a solution containing the drug, followed by 3 μ L of the solution containing dithiothreitol (DTT). The final concentrations of PM2 DNA and DTT present in the reaction medium were 9.4×10^{-5} M and 0.45 mM, respectively. Concentrations of esp A₁: 0, 9.23×10^{-10} M; 1.38, 4.62, 9.23×10^{-9} M;

(7) Povirk, L.; Houlgrove, C. W.; Hau, J.-H. *J. Biol. Chem.* **1988**, *263*, 19263-19266.

(8) Campbell, V. W.; Jackson, D. A. *J. Biol. Chem.* **1980**, *255*, 3726-3735.

(9) Marky, L. A.; Breslauer, K. J. *Proc. Natl. Acad. Sci. U.S.A.* **1987**, *84*, 4359-4363.

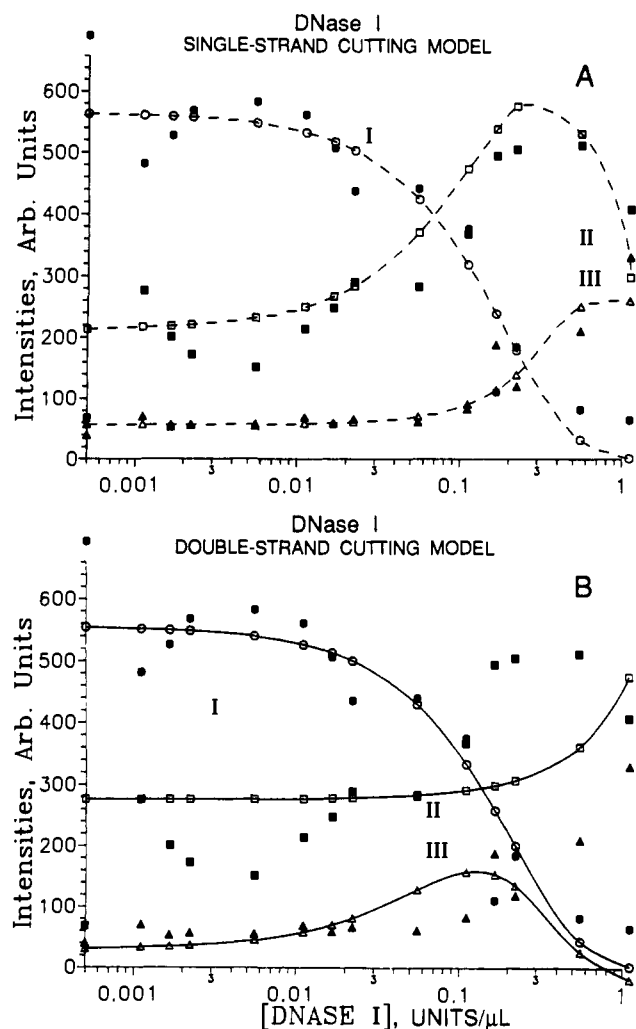


Figure 3. Intensities for forms I, II, and III DNA resulting from DNase I cleavage of PM2 DNA as a function of DNase I concentration. Intensities calculated by the single-strand (A) and double-strand (B) models described in the text are open symbols. Curves are fits to calculated intensities.

1.39, 1.85, 4.62, 9.23×10^{-8} M; 1.39, 1.87, 4.62×10^{-7} M. Concentrations of esp C: 0, 9.23×10^{-10} M; 1.85, 4.62, 9.23×10^{-9} M; 1.39, 1.85, 4.62, 9.23×10^{-8} M; 1.39, 1.85, 2.31, 4.62, 9.23×10^{-7} M. Concentrations of calicheamicin used in the study: 0, 9.69×10^{-9} M; 1.38, 4.62, 9.23×10^{-8} M; 1.85, 4.62, 9.23×10^{-7} M; 1.38, 1.85 $\times 10^{-6}$ M. After a digest time of 10 min, the reaction was terminated by the addition of $4 \mu\text{L}$ of a 3×10^{-3} M sodium dodecyl sulfate "stop" solution, and the DNA was loaded onto a horizontal 0.8% agarose gel and electrophoresed. After electrophoresis, the gel was soaked in a $0.5 \mu\text{g}/\text{mL}$ solution of ethidium bromide for 1 h, placed on a UV transilluminator, and photographed with use of a Polaroid camera equipped with positive/negative Type 55 film. The resulting negative was "fixed" according to the manufacturer's recommendation with aqueous 18% Na_2SO_3 . A photograph of the stained gel for esp C is shown in Figure 2.

Cleavage of PM2 DNA was also carried out with use of DNase I in a total volume of $7 \mu\text{L}$ of the buffer 14.3 mM Tris-HCl/9.1 mM $\text{MgCl}_2/2.3$ mM CaCl_2 , pH 7.5. After proceeding for 10 min, the reaction was terminated by addition of aqueous EDTA and the products were loaded onto an agarose gel. Concentrations of DNase I (units/ μL) present in the various reactions: 1.1, 1.67, 2.22, 5.56×10^{-2} ; 1.1, 1.67, 2.22, 5.56×10^{-3} ; 1.1, 1.67, 2.22, 5.56×10^{-4} ; 1.1 $\times 10^{-6}$.

A Molecular Dynamics Model 300A microdensitometer capable of whole-spot integration was used to scan the photographic negatives of the agarose gel data. Control experiments (data not shown) showed that measured densities on the negative were dependent on the placement of the gel relative to the optical axis of the camera and to a certain extent on the gel's location on the UV transilluminator. The intensity varied smoothly from a maximum in the center of the negative to minima at both edges. In order to correct for these experimental effects as well as errors due to loading slightly different amounts of DNA into the wells of the gel, the sum of the intensities of the three DNA forms for each

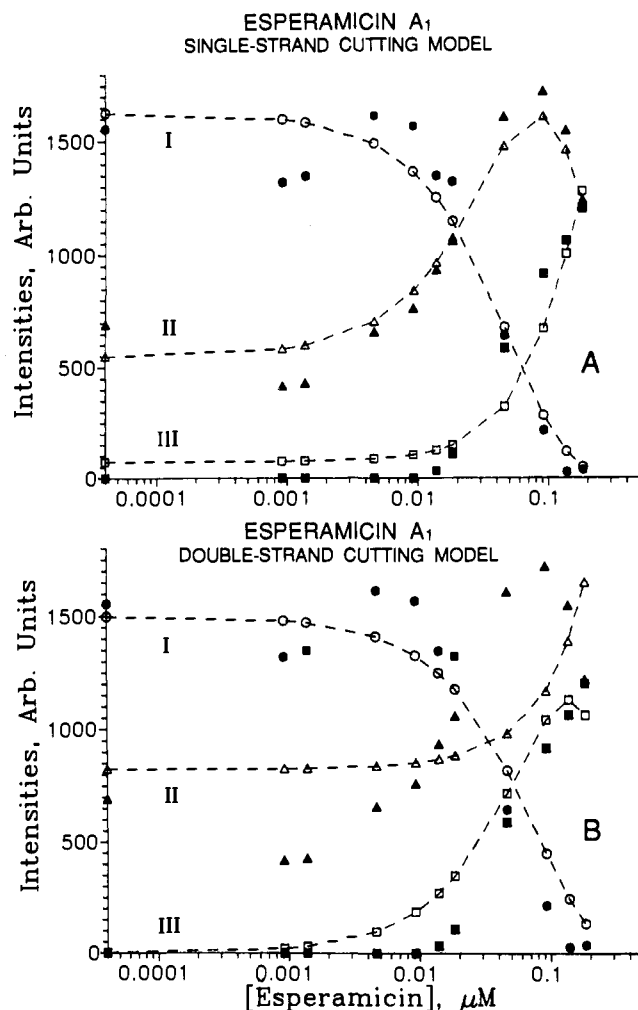


Figure 4. Intensities for forms I, II, and III DNA resulting from esperamicin A₁ cleavage of PM2 DNA as a function of concentration of esperamicin A₁. See caption to Figure 3 for further details.

lane was adjusted to a constant value. The maximum value of the correction factor was 1.9. Lanes for which this type of correction would not be valid, i.e., the lanes having the highest drug and DNase I concentrations, where significant amounts of short fragments were produced, were not used in the analysis. Although response of photographic film to ethidium bromide fluorescence has been reported to be nonlinear,¹⁰ no correction for this effect was made. Gels containing differing amounts of stained DNA but photographed so as to minimize the illumination/optic effects (see above) showed that any nonlinearity was minor over the density range studied. Because of its superhelical nature, the ability of form I DNA to stain under saturated ethidium bromide conditions was less than that of forms II and III DNA: the earlier determined factor of 0.8 was used to multiply calculated intensities of form I DNA (see below).¹¹ The experimental band intensities as a function of drug concentration or units (DNase I) can be found in Figures 3–6.

The band intensities are proportional to the amounts of the various forms of DNA present at the end of the digest period τ (10 min). The kinetic models for the interconversion of the various forms of DNA are discussed in the next section. Given such a model, one can calculate the amount of each DNA form for each concentration of cleavage agent, in terms of the rate constants and the amounts of the three forms present before reaction with cleavage agent. The rate constants and initial amounts are parameters determined by seeking the values that minimize the deviation between the experimental and calculated band intensities. Thus, if I_{ij} is the intensity of form i at $t = \tau$ when the cleavage agent concentration is c_j and if I_{ij}^{calc} is the corresponding value calculated according to a model, we minimize

$$D = \sum_i \sum_j (I_{ij} - I_{ij}^{\text{calc}})^2$$

(10) Prunell, A.; Strauss, F. and Leblanc, B. *Anal. Biochem.* 1977, 78, 57–65.

(11) Bauer, W.; Vinograd, J. *J. Mol. Biol.* 1968, 33, 141–171.

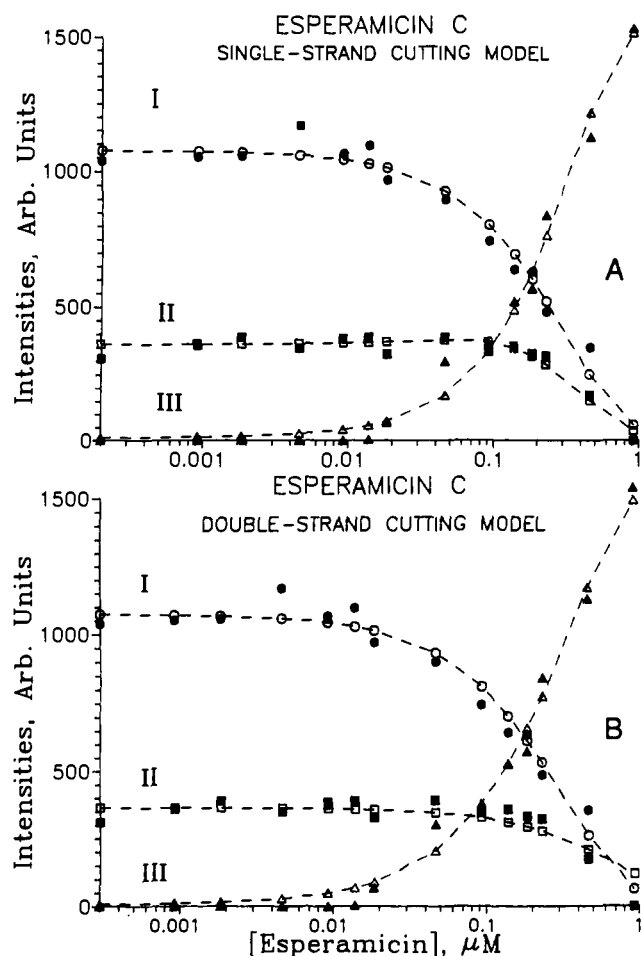


Figure 5. Intensities for forms I, II, and III DNA resulting from esperamicin C cleavage of PM2 DNA as a function of concentration of esperamicin C. See caption to Figure 3 for further details.

with respect to these parameters. The nonlinear minimization problem is solved by the Simplex Search Method.¹² With this iterative method, values of D are calculated for several sets of values of the parameters. The calculated values of D indicate in what way the parameters should be changed to obtain lower values of D , and the process is repeated.

Results and Discussion

In the cases of esperamicin and calicheamicin, an activation agent has been postulated to produce a diradical possessing two DNA-damaging equivalents. If both radicals on the phenylene moiety reach DNA targets, strand scission will be a two-step kinetic process with reaction of one radical with a site on DNA, e.g., removing a hydrogen atom from deoxyribose, followed by the reaction of the second radical with another DNA site. (The likelihood of a concerted process, i.e., identical reaction rates for the reaction of the two radicals, seems low since it would require optimal positioning of both radicals relative to their respective DNA targets.) If the drug did not move from its original position in the time required for both radicals of the phenylene moiety to react with DNA targets on opposing strands, the covalently closed circular form I DNA would be converted directly to form III DNA without passing through the nicked circular form II DNA. Although the rate constant of hydrogen atom abstraction of the phenylene diradical of esperamicin and calicheamicin from a donor has not been measured, studies on related systems suggest that this constant is large, $\sim 10^6 \text{ M}^{-1} \text{ s}^{-1}$, and thus the drug may not have time to migrate to a new position on DNA before hydrogen abstraction from some source occurs.¹³ If only one of the phe-

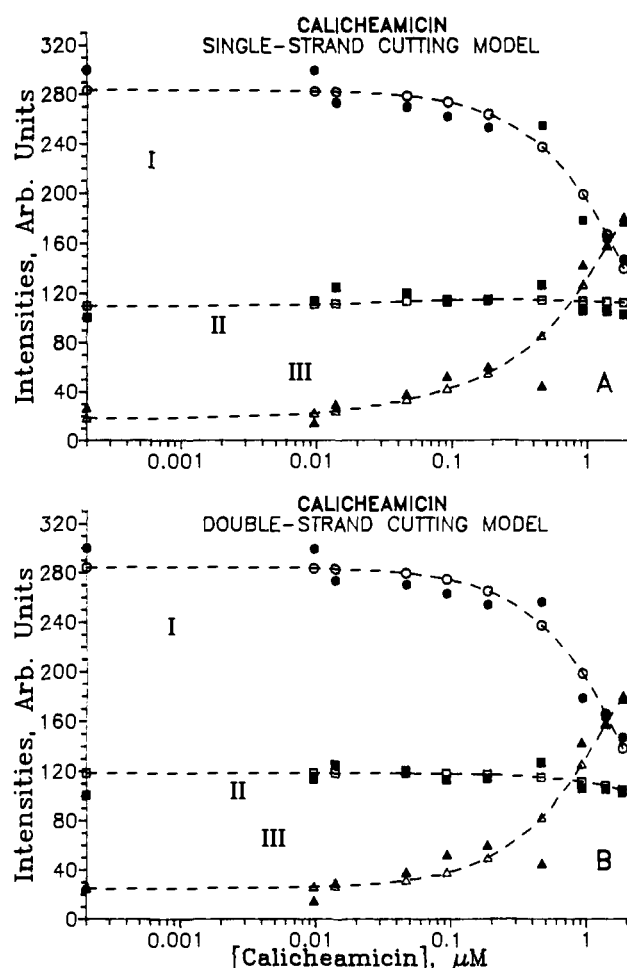


Figure 6. Intensities for forms I, II, and III DNA resulting from calicheamicin cleavage of PM2 DNA as a function of calicheamicin concentration. See caption to Figure 3 for further details.

nylene diradicals reacts with DNA or both react with the *same* strand of the polymer, form I would convert to form II DNA. Extensive random cleavage of the latter form would eventually produce the linear product, form III DNA.

The experimental results of the studies involving PM2 DNA are shown in Figures 2–6, solid symbols. In the cases of DNase I and esp A₁ (Figures 3 and 4), cleavage caused closed circular form I DNA to decrease in amount while at the same time nicked circular form II increased in amount. Higher concentrations of DNase I or esp A led to a decrease in the amount of form II while linear form III DNA increased in amount. This behavior contrasted with that of esp C and calicheamicin, which showed decreases in the amount of form I with concomitant increases in the amount of form III DNA (Figures 5 and 6). These intensity/concentration plots (Figures 3–6) were analyzed according to the single- and double-strand cleavage models given below. The calculated rate constants can be found in Table I.

To model the interconversion of the three forms of PM2 DNA, we begin by assuming that the rate of nicking of each form of DNA is proportional to its concentration and to the concentration of the cleavage agent (DNase I or drug). Each interconversion rate is proportional to the rate of nicking. Then, for example, the rate of decrease of the concentration of the closed circular form I DNA is $d[I]/dt = -k_1'[I][P]$ where k_1' is a second-order rate constant and $[P]$ is the concentration of cleavage agent. The experimental data for esperamicin and calicheamicin show that there is little or no change in the concentrations of the three forms of PM2 DNA over the digest time unless the drug concentrations exceed about $0.02 \mu\text{M}$. Since the concentration of PM2 DNA (plasmid per unit volume) is only $0.01 \mu\text{M}$, and since we believe almost all the drug is bound to the DNA, this implies that only a fraction of the drug is activated, so that the drug concentration

(12) Fletcher, R. *Practical Methods of Optimization*; Wiley: Chichester, 1980.

(13) Lockhart, T. P.; Comita, P. B.; Bergman, R. G. *J. Am. Chem. Soc.* **1981**, *103*, 4082–4090.

Table I. Rate Constants for Esperamicin, Calicheamicin, and DNase I Cleavage of PM2 DNA

cleavage agent	model ^a	k_1' ^b	k_4' ^b	k_2' ^b	k_3' ^b	$D \times 10^5$ ^c
DNase I ^d	ss	0.49 ± 0.07		0.09 ± 0.03	0.11 ± 0.03	1.4
DNase I ^d	ds		0.46 ± 0.20	-0.05 ± 0.03	0.10 ± 0.05	4.5
esp A ₁	ss	1.95 ± 0.25		0.50 ± 0.07	0.07 ± 0.08	6.9
esp A ₁	ds		1.31 ± 0.21	-0.38 ± 0.06	-0.11 ± 0.10	20.4
esp C	ss	0.31 ± 0.03		0.94 ± 0.10	0.09 ± 0.007	1.2
esp C	ds		0.31 ± 0.03	0.12 ± 0.04	0.00 ± 0.01	1.4
calicheamicin	ss	0.038 ± 0.004		2.51 ± 1.5	0.015 ± 0.010	0.047
calicheamicin	ds		0.039 ± 0.004	0.007 ± 0.003	0.019 ± 0.009	0.046

^a Model ss involves only single-strand cleavage, i.e., form I → form II → form III DNA. Model ds is for double-strand cleavage, form I → form III and form II → form III. ^b Second-order rate constants in $\mu\text{M}^{-1} \text{min}^{-1}$. ^c The quantity D is the sum of the squared deviations between experimental and calculated data. Stated errors are changes producing 10% increase in D . ^d For DNase I, the rate constants are in $(\text{units/L})^{-1} \text{min}^{-1}$.

[P] remains essentially constant during the time of the digest. Therefore, all the rate laws are pseudo-first-order. For instance, we write $d[\text{I}]/dt = -k_1[\text{I}]$, where the pseudo-first-order rate constant k_1 is k_1' multiplied by [P].

Single-Strand Cleavage Model. We first consider that the nicking process converts closed circular DNA, form I, to nicked circular DNA, form II, with a rate constant of k_1 . Subsequent nicking converts form II to linear DNA (form III) with a rate constant of k_2 . Further cleavage of form III converts it to undetected forms of DNA with a rate constant of k_3 (including all processes that destroy form III DNA). The rate laws are then

$$\frac{d[\text{I}]}{dt} = -k_1[\text{I}] \quad \frac{d[\text{II}]}{dt} = k_1[\text{I}] - k_2[\text{II}]$$

$$\frac{d[\text{III}]}{dt} = k_2[\text{II}] - k_3[\text{III}]$$

Integrating these expressions, we have

$$[\text{I}] = C_0 e^{-k_1 t} \quad (1)$$

$$[\text{II}] = \frac{k_1 C_0}{k_2 - k_1} e^{-k_1 t} + \left(N_0 - \frac{k_1 C_0}{k_2 - k_1} \right) e^{-k_2 t} \quad (2)$$

$$[\text{III}] = \alpha e^{-k_1 t} + \beta e^{-k_2 t} + (L_0 - \alpha - \beta) e^{-k_3 t} \quad (3)$$

where $\alpha = k_1 k_2 C_0 (k_2 - k_1)^{-1} (k_3 - k_1)^{-1}$ and

$$\beta = k_2 \left(\frac{-k_1 C_0}{k_2 - k_1} + N_0 \right) (k_3 - k_2)^{-1}$$

Here, C_0 , N_0 , and L_0 are, respectively, the initial values of [I], [II], and [III]. The DNA used in this investigation included forms II and III DNA in addition to form I DNA so N_0 and L_0 are not zero. For t in these expressions we will use the digest time τ (10 min), and for k_i , the true rate constant, k_i' multiplied by the concentration of cleavage agent.

Double-Strand Cleavage Model. Another possibility is that the cleavage agent, nicking the closed circular DNA, converts it directly to the linear form, i.e., form I → form III. This is termed a double-strand break. The rate laws are then

$$\frac{d[\text{I}]}{dt} = -k_4[\text{I}] \quad \frac{d[\text{II}]}{dt} = -k_2[\text{II}]$$

$$\frac{d[\text{III}]}{dt} = k_4[\text{I}] + k_2[\text{II}] - k_3[\text{III}]$$

The linear form can be produced from the nicked form, or directly from form I. Integrating these equations, we obtain

$$[\text{I}] = C_0 e^{-k_4 t} \quad (4)$$

$$[\text{III}] = N_0 e^{-k_2 t} \quad (5)$$

$$[\text{III}] = \alpha e^{-k_4 t} + \beta e^{-k_2 t} + (L_0 - \alpha - \beta) e^{-k_3 t} \quad (6)$$

where C_0 , N_0 , and L_0 are the initial concentrations of the three forms and

$$\alpha = k_4 C_0 / (k_3 - k_4) \quad \beta = k_2 N_0 / (k_3 - k_2)$$

There are, as in the previous model, six parameters: three rate constants and three initial concentrations.

Derivation of Rate Constants. For either of the two models, the amounts or intensities of all three forms may be calculated for all drug or DNase I concentrations in terms of six parameters: three rate constants and three initial concentrations (C_0 , N_0 , L_0). For any set of values for these parameters, calculated intensities may be compared with the experimental intensities. The parameters are varied to minimize the sum of the squared deviations: $D = \sum (I_{ij} - I_{ij}^{\text{calc}})^2$. Here, I_{ij} is the intensity of form i when the drug or DNase I concentration is c_j . The values of the second-order rate constants found by minimization of D , for each model and for each cleavage agent, are given in Table I, along with the minimum values of D . In Figures 3–6, we show the intensities calculated according to the models, using the best values for the parameters (open symbols).

Comparison of the values of D for different models shows whether one model is significantly better than another, or whether the two fit the experimental data equally well. How well the experimental data are fit may also be judged from Figures 3–6 themselves. Comparison of rate constants helps in understanding the physical meaning of the models. Due to the fact that the DNase I concentration is expressed in units and the drug concentration in moles per liter, the rate constants for the enzyme and drug are not directly comparable. However, comparing the ratios of rate constants is valid. It should be noted that the value of k_3' , the rate constant for conversion of form III DNA to shorter fragments, cannot be determined accurately from the data, because the data are for low drug concentrations, for which the amount of short fragments produced is small.

DNA Cleavage Mechanism. DNase I. Prior to analyzing the cleavage data for esperamicin and calicheamicin using the outlined coupled kinetic approach, we analyzed cleavage of PM2 DNA by the enzyme DNase I. This enzyme binds and cleaves DNA by a well-known mechanism and, under the conditions used in the study, should cleave via a single-strand process.^{8,14} DNase I is a 30-kDa protein that hydrolyzes the phosphodiester backbone of DNA. Single-crystal X-ray analysis has shown that, when DNase I is bound to DNA, the calcium ion at the catalytic site of the enzyme is positioned near a phosphate group on one strand of DNA.¹⁴ The metal ion acts as a Lewis acid and, when bound to the phosphate group, facilitates the hydrolysis of the diester linkage of DNA.

Table I shows that the single-strand model fits much better than the double-strand model. The ratio of k_1' to k_2' for this model is ~ 5.4 . If the affinities of DNase I for all three forms of PM2 DNA were the same and cleavages were completely random on both strands, the ratio k_1'/k_2' would be expected to be 2 orders of magnitude greater than that found. This estimate is based on the length of the PM2 DNA genome, 9300 nucleotides, and the assumption that the formation of form III from form II requires cleavages on opposing strands, which are within 6–10 base pairs of each other. The lower than expected ratio can be due to an unusually low value of k_1' and/or a large value of k_2' . In other studies with radiolabeled restriction fragments in the presence of

a closed circular DNA as a carrier, it is evident that the affinity of DNase I for the closed circular DNA is much less than its affinity for linear DNA, e.g., calf thymus DNA.¹⁵ Since the enzyme must bind in order to cleave DNA, this suggests that k_1' , for cleavage of the closed circular form, will be lower than expected (due to lower affinity for closed circular DNA). The enzyme may also cause some double-strand cleavage of DNA, as has been shown to occur in the presence of Mn^{2+} and Co^{2+} .⁸ In the context of the single-strand cleavage model this would lead to a higher value of k_2' , thus also lowering the ratio k_1'/k_2' . Although a model including both single- and double-strand cleavage could be used, it is unnecessary since a simple, single-strand cleavage model already fits the data within experimental error. It may be noted that k_2' and k_3' are about the same size, suggesting that the process of conversion of form II is similar to the process of destruction of form III.

As shown in Table I and Figure 3, analysis of the data according to the double-strand cleavage model leads to a significantly poorer fit to the experimental intensities than using the single-strand model. This implies that the former model is not applicable and DNase I cleaves DNA primarily via a single-strand cleavage process. Further evidence for this conclusion is the appreciable negative (and thus unacceptable) value of k_2' with the double-strand cutting model.

Esperamicin A₁. The single-strand cleavage model fits the data for this esperamicin analogue, as shown in Table I and Figure 4. An attempt to fit them with the double-strand model led to a 3-fold increase in the sum of the squared deviations, D , and to a substantial negative value of k_2' , showing that esp A₁ is mainly a single-strand cleavage agent. The ratio k_1'/k_2' for esp A₁ for the single-strand model is strikingly similar to that for DNase I (Table I). Because of the dramatic differences in structure and cleavage mechanism between the drug and the enzyme, this result was not expected. Like the enzyme, the drug may have a significantly reduced affinity for the tense form I DNA relative to the other two forms, which would lower the value of k_1' . Although the drug¹⁶ and the enzyme¹⁴ both cleave DNA from its minor groove, the drug is not likely to be as sensitive as the enzyme to the nuances of DNA structure. For example, changes in minor-groove width such as would occur between supercoiled form I and relaxed forms II and III DNA would be expected to affect drug binding to a lesser extent than enzyme binding. The fact that k_1'/k_2' is lower than expected for random single-strand cleavage may also reflect a certain number of double-strand cleavages occurring with esp A₁. In the context of the single-strand model this would cause a higher value of k_2' and lower the ratio k_1'/k_2' . DNA cleavage by the drug, unlike the enzyme, is not expected to be catalytic. The activation mechanism requires the formation of a phenylene diradical that reacts with hydrogen atom donors in an irreversible manner, ultimately forming the aromatized drug esp Z. Esperamicin Z is not capable of cleaving DNA.²

The single-strand cleavage behavior of esp A₁ means that one of the radicals of the phenylene diradical is unproductive with regard to a detectable strand break in the assay used. Although further study is warranted, it may be that the "silent" radical reacts with solvent, the drug itself, or DNA. If the reaction with DNA involved the cleaved strand or the opposing strand but the hydrogen atom abstraction did not lead to a break in the sugar-phosphate backbone of the strand, form I would not convert directly to form III DNA. It may be noted that k_2' is much bigger than k_3' for esp A₁. The reason for this is not understood, but our data show that, even at the highest esperamicin concentration, the concentration of form III DNA is still rising, which makes the determination of k_3' from these data problematic.

Esperamicin C and Calicheamicin. Figures 5 and 6 and Table I show that the cleavage behavior of esp C and calicheamicin is significantly different from that of esp A₁ or DNase I. The sum

of the squared deviations, D , in Table I shows that both models, single strand and double strand, fit the data for esp C and calicheamicin equally well. The fact that both models fit can be understood by considering the values of k_1' and k_2' for the single-strand model. With $k_2' > k_1'$ in this model, almost every initial break in a form I DNA species, converting it to form II, is quickly followed by the conversion of form II to form III. This makes the overall process effectively a double-strand or "simultaneous" cleavage event: there is very little net production of form II because it is immediately converted to form III. That this is indeed what is happening may be seen by comparing the calculated intensities for the two models (dashed lines and open symbols in Figures 5 and 6). The curves are practically identical, meaning that the single-strand model is equivalent to the double-strand model for this choice of parameters.

Obviously, one cannot conclude that double-strand cleavage is occurring to the exclusion of single-strand cleavage. Both probably take place, and one could construct a model including both processes I → II and I → III. Such a model would have an additional parameter (a rate constant). Since the present six-parameter models fit the data satisfactorily, fitting to a seven-parameter model does not seem a reasonable procedure. The value of D would certainly decrease, but the values of the parameters determined would not be very meaningful.

In the double-strand cleavage model, the fact that k_2' is much less than k_4' implies that the formation of form III from form I is faster than its formation from form II. In the single-strand cleavage model, the ratio k_2'/k_1' reflects the ratio of the rate of II → III to the rate of I → II, large values of this ratio signifying more effective double-strand cleavage. Since $k_2'/k_1' \approx 3$ for esperamicin C and 66 for calicheamicin, we conclude that the latter is more efficient at causing double-strand breaks. From the values of k_1' it is also evident that the rate of cleavage of closed circular form I DNA by calicheamicin is 1 order of magnitude less than that of esperamicin C and almost 2 orders less than that of esperamicin A₁. Whether this is due to differences in the cleavage rate constants for the compounds or simply a manifestation of differing affinities that the agents may have for DNA remains to be determined. However, from the rate data it is clear that once calicheamicin cleaves one strand of DNA, cleavage of the opposing strand is rapid.

Although it is not possible to identify the relative locations of the two breaks in DNA from the agarose gel studies, earlier work using sequencing methods showed that calicheamicin-induced breaks are three nucleotides apart and skewed in the 3'-direction along the strand.⁴ This indicates that the drug is bound in the minor groove and, as has been recently shown in modeling studies,¹⁷ with the warhead portion straddling two base pairs of DNA. Recent NMR studies¹⁸ have further indicated that the sugars of calicheamicin are "preorganized" and that they adopt a conformation outside of DNA closely matching that of the minor groove. Although less is known about the binding of esperamicin to DNA, the skewing in the drugs' cleavage patterns² and the ability of certain other drugs¹⁶ to influence DNA cleavage by esperamicin indicate that this compound also binds in the minor groove. The work presented here clearly shows that for esp C the warhead portion of the drug is situated such that targets on both strands are readily accessible and that double-strand cleavage occurs with high probability when compared to esp A₁. It is interesting to note that double-strand cleavage occurs with the two compounds having a single point of attachment between the oligosaccharide and the 1,5-diyne-3-ene chromophore, e.g., esperamicin C and calicheamicin. Models (CPK) show that in the case of esperamicin A₁, which has substituents on two positions of the warhead, the deoxyfucose and the attached anthranilate residue can be proximal to one of the radicals of the phenylene diradical. Although additional model building involving energy minimization will be nec-

(15) Dabrowiak, J. C.; Goinga, H. Unpublished results.

(16) Sugiyama, Y.; Uesawa, Y.; Tokahashi, Y.; Kuwahara, J.; Golik, J.; Doyle, T. W. *Proc. Natl. Acad. Sci. U.S.A.* **1989**, *86*, 7672.

(17) Hawley, R. C.; Kiessling, L. L.; Schreiber, S. L. *Proc. Natl. Acad. Sci. U.S.A.* **1989**, *86*, 1105-1109.

(18) Walker, S.; Valentine, K. G.; Kahne, D. *J. Am. Chem. Soc.* **1990**, *112*, 6428-6429.

essary, this suggests that "self-quenching" by the drug of one of the radicals may be the reason that esp A₁ cleaves DNA in a single-strand manner.

Certain of the steps leading to the activation of the warhead portion of calicheamicin have recently been investigated by NMR methods.¹⁹ The first-order rate constant for the formation of aromatized drug from the Michael addition product outside of DNA is $5 \times 10^{-4} \text{ s}^{-1}$. In addition to being second-order rate constants, the k_i' in Table I involve all of the individual steps including drug activation and the processes on DNA leading to strand breakage and thus cannot be directly compared with the rate constants of microsteps measured by NMR.

Esperamicin C and calicheamicin are unique in their DNA cleavage mechanisms. A single activation event on their chromophores leads to a double-strand break in DNA. This behavior is different from that of neocarzinostatin, which although it breaks one strand and modifies the second strand requires posttreatment of the DNA in order to produce a double-strand break.^{5,7} Since

esp A₁ is more potent as an antitumor agent than is esp C,² single-versus double-strand cleavage is not the only factor influencing cytotoxicity. Cellular uptake and drug delivery very likely also play major roles in determining the biological effectiveness of the agents.

Conclusions

By using a coupled kinetic model, we studied the ability of esperamicin, calicheamicin, and the enzyme DNase I to cause single- or double-strand cleavage of DNA. The analysis shows that DNase I and esperamicin A₁ cleave DNA mainly via a single-strand process, whereas esperamicin C and calicheamicin cleave mainly through a double-strand mechanism. Examination of the structure of the drugs shows that the location of the sugars on the warhead portion of the agents is a factor influencing single-versus double-strand cleavage of DNA.

Acknowledgment. We thank Drs. Golik and T. Doyle of Bristol-Myers Squibb Co. and G. Ellestad of Lederle Laboratories for helpful discussions concerning this work. We also thank the American Cancer Society, Grant NP-681, and Bristol-Myers Squibb Co. for financial support of the research.

(19) De Voss, J. J.; Hangeland, J. J.; Townsend, C. A.; *J. Am. Chem. Soc.* **1990**, *112*, 4554-4556.

Humidity-Controlled Reversible Structure Transition of Disodium Adenosine 5'-Triphosphate between Dihydrate and Trihydrate in a Single Crystal State

Yoko Sugawara,*† Nobuo Kamiya,† Hitoshi Iwasaki,† Tetsuzo Ito,† and Yoshinori Satow‡

Contribution from RIKEN (The Institute of Physical and Chemical Research), Wako, Saitama 351-01, Japan, the Kanagawa Institute of Technology, Atsugi, Kanagawa 243-02, Japan, and the Photon Factory, National Laboratory for High Energy Physics (KEK), Tsukuba, Ibaraki 305, Japan. Received May 15, 1990

Abstract: The humidity-controlled single-crystal transition of disodium adenosine 5'-triphosphate (Na₂ATP) between the dihydrate (1) and trihydrate (2) forms was investigated over the humidity range 5–50% at 23 °C by X-ray analysis. A crystal of 2 formed at high humidity changes into 1 at low humidity. The transition is reversible. The crystal structure of 1 was determined to be orthorhombic space group *P*2₁2₁2₁ with the cell parameters *a* = 27.572 (5), *b* = 21.066 (3), and *c* = 7.0854 (9) Å. The structure was solved by direct methods and refined to the final *R* value of 0.097 for 2450 independent reflections. Two water molecules, which are hydrogen-bonded to the hydroxyl groups of riboses in 2, are lost in 1. The triphosphate linkages are in helical arrangement, and the adenine bases are highly stacked along the *c* axis, as for 2. There are two ATP molecules, A and B, in an asymmetric unit. The conformation of molecule A in 1 resembles that in 2; the ribose is C3'-endo, and the exocyclic C4'-C5' torsion is gauche⁺. In molecule B, the ribose is C4'-endo, and the C4'-C5' torsion is gauche⁻, in contrast to C2'-endo-C3'-exo, and gauche⁺ in 2. The torsional angles around the P-O ester bonds of the triphosphate chains of both molecules in 1 differ from those in 2 by 8–47°. Conformational flexibility of ATP makes the single-crystal transition possible. The conformation of molecule B in 1 relates to the conformation of ATP in its complexes with enzymes. The crystal structure of 2 (Kennard; et al. *Proc. R. Soc. London* **1971**, *A325*, 401-436) was refined to the final *R* value of 0.117 with the newly collected data, and the original assignment of Na4 and OW4 was interchanged.

Introduction

Adenosine 5'-triphosphate (ATP)-enzyme interactions have been discussed with regard to the crystal structures of enzyme-ATP (or ATP analogue) complexes.¹⁻⁵ For example, in a series of site-directed mutagenic studies of tyrosyl-tRNA synthetase (TyrTS), the crystal structure of the TyrTS-tyrosyl adenylate complex was referred to in order to analyze the ATP-TyrTS interactions.³ Although the concept of a "rigid" nucleotide was proposed based on conformational analyses of the crystal structures

of nucleotides,⁶ the adenosine moiety of ATP-enzyme complex is sometimes in an "uncommon" conformation; the ribose of the

(1) (a) Montellhet, C.; Blow, D. M. *J. Mol. Biol.* **1978**, *122*, 407-417. (b) Rubin, J.; Blow, D. M. *J. Mol. Biol.* **1981**, *145*, 489-500. (c) Brick, P.; Blow, D. M. *J. Mol. Biol.* **1987**, *194*, 287-297.

(2) (a) Banks, R. D.; Blake, C. C. F.; Evans, P. R.; Haser, R.; Rice, D. W.; Hardy, G. W.; Merrett, M.; Phillips, A. W. *Nature* **1979**, *279*, 773-777. (b) Watson, H. C.; Walker, N. P. C.; Shaw, P. J.; Bryant, T. N.; Wendell, P. L.; Fothergill, L. A.; Perkins, R. E.; Conroy, S. C.; Dobson, M. J.; Tuite, M. F.; Kingsman, A. J.; Kingsman, S. M. *EMBO J.* **1982**, *1*, 1635-1640.

(3) Shoham, M.; Steitz, T. A. *J. Mol. Biol.* **1980**, *140*, 1-14.

(4) (a) Sachsenheimer, W.; Schulz, G. E. *J. Mol. Biol.* **1977**, *114*, 23-36. (b) Pal, E. F.; Sachsenheimer, W.; Schirmer, R. H.; Schulz, G. E. *J. Mol. Biol.* **1977**, *114*, 37-45. (c) Fry, D. C.; Kuby, S. A.; Mildvan, A. S. *Biochemistry* **1985**, *24*, 4680-4694.

*RIKEN.

†Kanagawa Institute of Technology.

‡KEK. Present address: Faculty of Pharmaceutical Sciences, University of Tokyo, Hongo, Bunkyo, Tokyo 113, Japan.